Journal of Materials Chemistry C

Accepted Manuscript

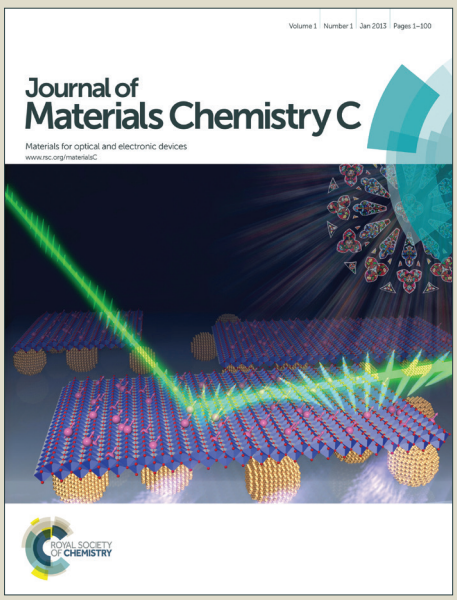

ROYAL SOCIETY OF CHEMISTRY

www.rsc.org/materialsC

Polarized and Non-polarized Photoluminescence of $GaInP_2$ Alloy with Partial CuPt-type Atomic Ordering: Ordered Domains vs. Disordered Regions

J. Q. Ning, S. J. Xu,* Z. Deng, and Z. C. Su

Polarized photoluminescence (PL) spectroscopy was employed to conduct an in-depth investigation into electronic structures and optical properties of $GaInP_2$ alloy with spontaneous atomic ordering. By examining variable-temperature polarized PL spectra in detail, it was found that the luminescence from $GaInP_2$ is composed of two components: polarized and non-polarized parts. These two components exhibit dissimilar temperature dependence. The former is ascribed to the emission of carriers localized in the ordered domains while the latter to the emission of carriers localized in the disordered regions. Thermal activationand transfer of localized carriers from the ordered domains to the disordered regions was revealed and characterized with a thermal activation energy of 10 meV.

Key Words: $GaInP_2$ alloy, polarized photoluminescence, spontaneous atomic ordering, carrier localization

Department of Physics and HKU-Shenzhen Institute of Research and Innovation (HKU-SIRI), The University of Hong Kong, Pokfulam Road, Hong Kong, China.E-mail: sjxu@hku.hk

Introduction

$GaInP_2$ alloy has attracted considerable attention due to itsgreat applications in various optoelectronic devices such as light-emitting diodes,[1] lasers,[2] and high-efficiency solar cells.[3] In addition to its outstanding optoelectronic properties, this ternary III-V alloy possessesan interesting spontaneous ordering property that Ga and In atoms distribute on alternating {111} lattice planes to form a superlattice-like structure. This CuPt-type ordering reduces the lattice symmetry ordering and may strongly alter electronic and optical properties of alloys. The resulting apparent effects include band-gap reduction, valence-band splitting and optical anisotropy.[4] It has been widely recognized that CuPt-type ordering in III-V alloys can be significantly affected by growth conditions such as V/III radio, growth temperature and growth rate, and different degrees of long-range ordering can be obtained by varying growth conditions. Under a given growth condition, a certain degree of ordering can only be obtained in a statistical manner, which means that we cannot expect an entire alloy lattice with the same degree of ordering. Instead, $GaInP_2$ alloys contain a statistical distribution of domains with varying degrees of ordering,[5,6] which has been confirmed by spatially resolved PL measurements.[7]

For the spontaneously ordered $GaInP_2$ alloys, extensive theoretical and experimental studies have been conducted to investigate the ordering-induced properties such as band-gap reduction and valance-band splitting,[5,8,9] optical anisotropy,[10] and polarization electric fields inside ordered domains.[11] Among them, optical anisotropy is a very attractive subject. Actually, it involves two types of anisotropy in optical transitions, namely, absorption anisotropy and emission anisotropy. Absorption anisotropy is a phenomenon of absorption coefficient depending on the polarization of incident light and different optical transitions can only be excited by light with defined polarization states. This allows one to measure the band structure of ordered $GaInP_2$ by varying the polarization of incident light in the measurements of absorptionspectroscopy or photoluminescence excitation (PLE) spectroscopy.[5,12,13] Emission anisotropy manifests itself as the emission of an inherently polarized light along the ordering planes in ordered $GaInP_2$ alloy, which is usually observed in polarized photoluminescence measurements.[14] The origin of emission anisotropy was essentially attributed to the valence-band splitting effect resulting from reduced crystal symmetry in CuPt-type ordered $GaInP_2$ alloy.[15] However, the sole valence-band splitting effect could not interpret all the spectral features observed from polarized PL experiments. For instance, usually measured PL spectra from $GaInP_2$ alloys are significantly broadened, and besides the intensity dependence on polarization directions, the spectral lineshape also shows substantial dependence on polarization. The latter phenomenon has been paid few attentions to so far. In this article we present an in-depth study on the polarized PL spectra in a $GaInP_2$ alloy with partially CuPt-type ordering. It was found that the emission spectra of the $GaInP_2$ alloy actually contain both polarized (p-PL) and non-polarized (np-PL) components, corresponding to the emissions of carriers in ordered and disordered domains in the

sample, respectively. These two PL components show different temperature-dependent behaviors.

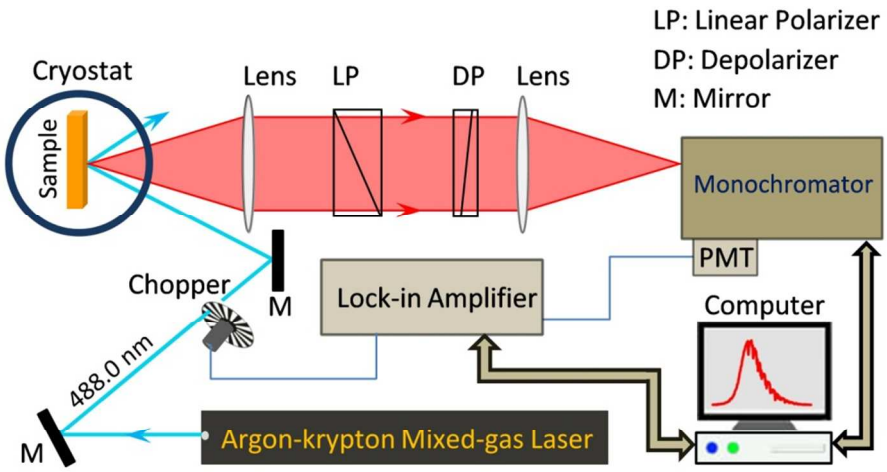

Fig. 1 Experimental arrangement for polarization-dependent PL measurements.

Experimental details

In this study, the $GaInP_2$ thin film was grown on a GaAs (001) substrate with metalorganic vapor phase epitaxy. The substrate temperature during epitaxy growth was 700 ^{o}C while the V/III gas-flow ratio was maintained at 200. The polarized PL measurements were performed on a variable-temperature PL setup which was described elsewhere.[16] The 488.0 nm line from an argon-krypton mixed-gas laser was employed as the excitation light source. A linear polarizer was used for the PL polarization analysis, and a depolarizer was followed to minimize the dependence of grating diffraction efficiency on light polarization. Such experimental arrangement for polarized PL measurements was schematically drawn in Fig. 1. For the PL polarization analysis, we define $E_{\parallel}$ as the arrangement that the polarization plane is parallel to [110] crystallographic direction which is along the CuPt-type ordering plane of the $GaInP_2$ sample, and $E_{\perp}$ parallel to $[1\bar{1}0]$ direction. For the variable-temperature polarized PL measurements, the sample was mounted on the cold finger of a Janis closed cycle cryostat providing a varying temperature range of 4K-300K.[16]

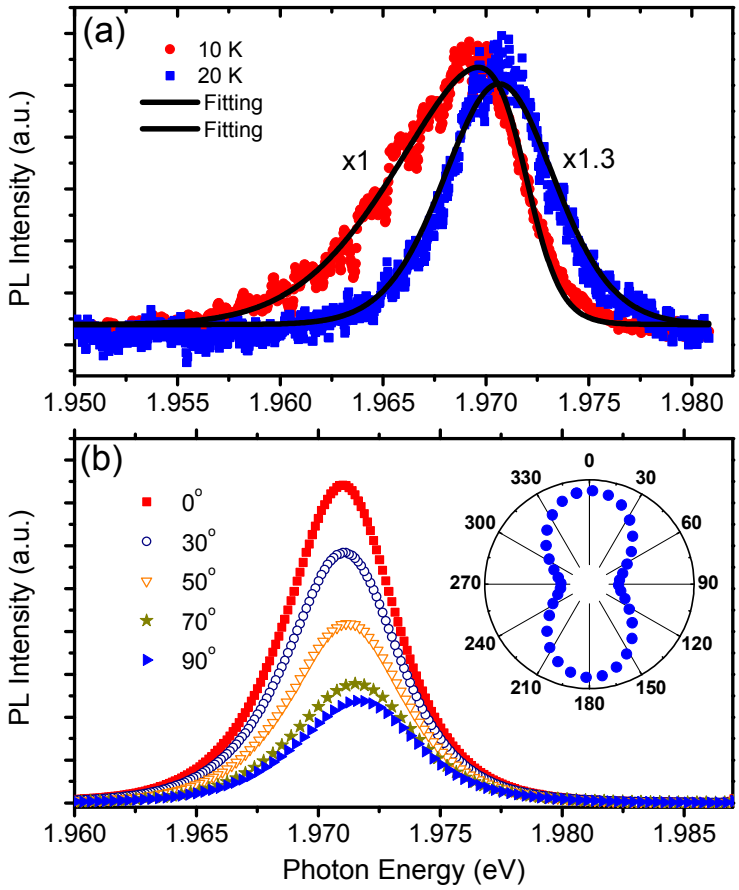

Fig. 2 (a) PL spectra (symbols) measured at 10 K and 20 K without polarization arrangement whenthe sample was excited with a 488.0 nm laser light at 0.1 μW. The solid lines are the theoretical fitting curves with a localized-state ensemble luminescence model; (b) PL spectra measured at 4 K and different polarization angles, while the laser power was 50 mW. The inset is the PL peak intensity at 1.971 eV vs. the polarization angle.

Results and discussion

We start our discussion from examining the characteristic PL spectra measured from the $GaInP_2$ sample without exerting the polarization arrangement. Fig.2(a) shows the typical PL spectra (symbols) acquired from the sample at the temperature of 10 K and 20 K, respectively, under the excitation of 488.0 nm laser line at 0.1 μW. The 10 K PL spectrum shows an asymmetric lineshape, i.e., having a broader band tail at the lower energy side. This type of spectral feature is consistent with the anti-Stokes PL spectrum of the $GaInP_2$ sample in our previous experimental investigation,[17] indicating the nature of localized-state ensemble luminescence. When the temperature is increased to 20 K, a

small but clear blue shift of the PL band is observed. At the same time, the spectral lineshape becomes symmetric. This is due to the effect of thermal redistribution of the photoexcited carriers within the localized states.[17,18] According to the localized-state ensemble luminescence model, the steady-state luminescence of localized carriers can be described by[18]

$$I_{PL}(E,T) \propto \rho(E) \cdot f(E,T) = \rho_0 e^{-(E-E_0)^2/2\sigma^2} \cdot \frac{1}{e^{(E-E_a)/k_B T} + \tau_{tr}/\tau_r}, \qquad (1)$$

where $E = h\nu$ is photon energy, $\rho_0 e^{-(E-E_0)^2/2\sigma^2}$ represents a Gaussian-type density of states due to a natural localized state distribution in materials, E_a is an energy level depending on material and carrier's injection level, k_B is the Boltzmann constant, T is temperature, $1/\tau_{tr}$ is escaping rate of localized carriers for nonradiative decay, $1/\tau_r$ is radiative rate of localized carriers for luminescence. In Fig. 2(a), the solid lines are the fitting results with Eq. (1). Values of the main parameters adopted in the fitting were $E_0 = 1.9757eV$, $E_a = 1.9714eV$, $\sigma = 5.4meV$, $\tau_{tr}/\tau_r = 0.0088$. It can be seen that the theoretical fitting spectra are in good agreement with the experimental spectra at the two temperatures. This firmly indicates that the luminescence mechanism is indeed localized-carrier ensemble luminescence.

The emission nature of localized carriers is vital for understanding the polarized PL spectra of the $GaInP_2$ alloy. Fig.2(b) exhibits the polarized PL spectra measured at 4 K with a laser power of 50 mW for different polarization angles. The polarization angle is defined as the measure between the polarization direction of the linear polarizer and the $E_{\parallel}$ direction. Therefore, 0^o polarization angle corresponds to the $E_{\parallel}$ arrangement, and 90^o polarization to $E_{\perp}$ direction. A most dominant feature of these polarized PL spectra is the strong dependence of the emission intensity on polarization directions: strongest at $E_{\parallel}$ polarization and the weakest at $E_{\perp}$. The peak intensity for $E_{\parallel}$ is more than three times stronger than that for $E_{\perp}$. The PL intensity at the photon energy of 1.971 eV was plotted with respect to the polarization angle as depicted in the inset of Fig.2, clearly showing the strong PL anisotropy of the sample studied in this work. As mentioned earlier, this optical anisotropy is generally attributed to the valence-band splitting.[13,14,19,20] However, the remarkable dependence of the PL peak position (spectral center) on the polarization angle could not be explained along with this direction. As seen from the PL spectra in Fig.2(b), the spectrumfor $E_{\perp}$ polarization shows an apparent blue shift with respect to the $E_{\parallel}$ spectrum. Actually, this phenomenon also appeared in previous studies on polarized PL spectra of $GaInP_2$ alloys,[14,20] but its underlying physical origin remains untouched.

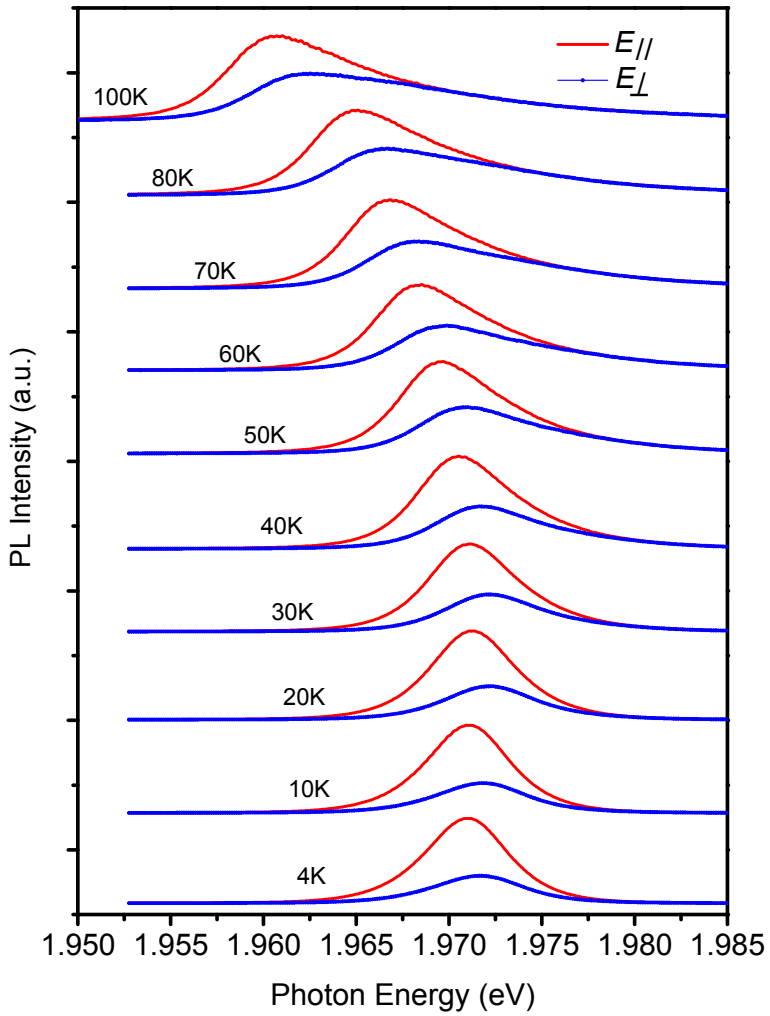

Fig. 3 Polarized PL spectra measured at different temperatures. For clarity, all the spectra were renormalized.

For probing the physical mechanism of the above-observed phenomenon, variable-temperature polarized PL spectra were measured and discussed below. For clarity, only the PL spectra measured at $E_{\parallel}$ and $E_{\perp}$ polarization configurations are depicted in Fig. 3 at different temperatures. By inspecting these spectra, we can see, below the temperature of 40 K, neither $E_{\parallel}$ nor $E_{\perp}$ emission exhibits observable red-shift with increasing temperatures. This could be due to the "compensation" effect between the blue-shift,

induced by the above-discussed thermal redistribution effect of the localized carriers within the localized states, and the band-gap shrinking caused by the temperature increment. When the temperature is increased to 40 K and above, noticeable red-shift of both the polarized and non-polarized emission bands takes place, indicating that the band-gap shrinking becomes dominant. In the meantime, noticeable change in lineshapes occurs for the two emission bands. Significant broadening occurs and the emission bands become more asymmetric, i.e., a long tail on the high energy side appears. This phenomenon can still be explained by the localized-state ensemble emission model. That is, more and more localized carriers gain thermal energy and occupy localized states at higher energy locations, leading to the asymmetric emission bands with long energy tails at the higher energy side. Besides these temperature-dependent behaviors, another two very prominent features can be also observed: i) the $E_{\parallel}$ and $E_{\perp}$ emissions get more separated in energy with increasing temperatures, i.e., their peak difference varies from ~0.6 meV at 4 K to >1.5 meV at 100 K; ii) the intensity of $E_{\parallel}$ emissions gets attenuated more quickly than that of $E_{\perp}$. For example, the integrated PL intensity ratio of $E_{\parallel}$ and $E_{\perp}$ is 2.95 at 4 K, and reduces to 1.42 at 100 K. These two remarkable behaviors of the polarized emission bands challenge the existing understandings and models such as the simple valence-band splitting mechanism.

To find out the underlying physics, we need to do an in-depth analysis to the variable-temperature spectral lines. By comparing the $E_{\parallel}$ and $E_{\perp}$ emissions at each temperature, one conclusion is apparent. That is, the most obvious difference in intensity between them appears at the lower energy side. In sharp contrast, the two bands exhibit analogous lineshapes at the higher energy side, especially tending to the identical lineshape at higher temperatures. This observation might provide an important clue for understanding the entire polarized PL spectra. From Fig. 2(b) and 3, we can see the characteristic of partially polarized light which can be considered to consist of a totally polarized and a totally non-polarized part.[21] The partially polarized light exhibits a maximum intensity in the direction of the polarization plane of the totally polarized part, which is the sum of the intensity of the polarized part and the non-polarized part in this direction, and a minimum intensity in the direction perpendicular to the polarization plane of the totally polarized part, exactly equal to the intensity of the non-polarized part in the perpendicular direction. Since non-polarized light has the same intensity (half of its total intensity) in any direction of its polarization planes, we thus can obtain the intensity of the polarized part by simply subtracting the minimum intensity from the maximum intensity. In the case of our experimental configuration, the maximum PL intensity is measured in the $E_{\parallel}$ direction, and the minimum intensity in the $E_{\perp}$ direction. We can therefore calculate the completely polarized PL spectrum ($I_{p\text{-}PL}$) by subtracting the PL spectrum ($I_{np\text{-}PL}$) measured at the $E_{\perp}$ direction from the PL spectrum (I_{tot}) at $E_{\parallel}$. That is, $I_{p\text{-}PL}=I_{tot}-I_{np\text{-}PL}$. By exerting this subtraction, the completely polarized PL spectra $I_{p\text{-}PL}$ are obtained and depicted as the thin line + open circlesin Fig.4(a) for several temperatures.

As seen from this figure, the $I_{p\text{-}PL}$ and $I_{np\text{-}PL}$ spectra show different temperature dependence. The $I_{p\text{-}PL}$ part is located at the lower energetic position and exhibits a monotonic red-shift as the temperature goes up. It also broadens at a much lower rate compared with the $I_{np\text{-}PL}$ counterpart, while its intensity drops relatively faster. On the contrary, the $I_{np\text{-}PL}$ spectra show non-monotonic temperature dependence for its peak position, and the spectra broaden at a higher rate and quickly transform into an asymmetric band with a strong higher-energy tail. This significant asymmetric broadening of the $I_{np\text{-}PL}$ part at higher energy side gives rise to a slower red-shift rate with increasing temperature. Therefore, the peak energy difference between the non-polarized and polarized components tends to be larger.

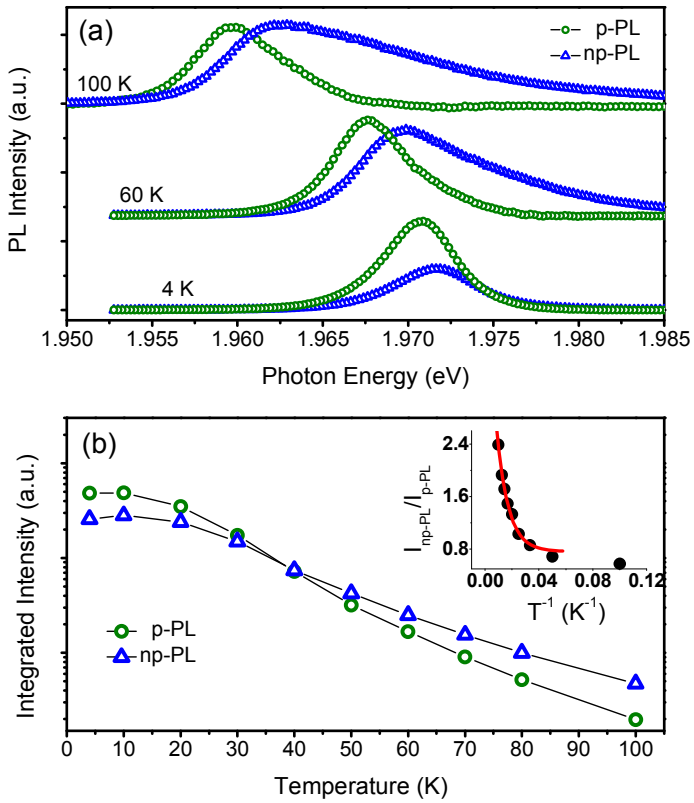

Fig. 4. (a) Normalized polarized (p-PL) and non-polarized (np-PL) PL spectra at 4 K, 60 K, and 100 K; (b) Temperature dependence of the integrated intensities of p-PL and np-PL bands. The inset depicts the fitting (solid line) to the integrated intensity ratio (solid circles) of $I_{np\text{-}PL}/I_{p\text{-}PL}$ by using eqn (2).

In order to explain these spectral features consistently and entirely, we propose a two-type localization state model in which the real-space potential profile is constructed with two groups of potential wells. It has been widely recognized that the spontaneously

ordered $GaInP_2$ samples are not uniformly ordered in real lattice and instead there exists a statistical distribution of domains with varying degrees of ordering.[5-7] Therefore, a real sample should be viewed as a matrix of disordered $GaInP_2$, embedded with ordered domains. For a highly ordered sample, it consists of a lot of large-size ordered domains with disordered components stuffed among them, and a disordered or less-ordered sample is a disordered lattice structure with small-sized ordered domains embedded inside. These disordered lattice and ordered domains certainly lead to different potential energy profiles and should be taken into account for understanding the observed optical and electronic properties of $GaInP_2$ alloy. Based on the experimental results and spectral analysis

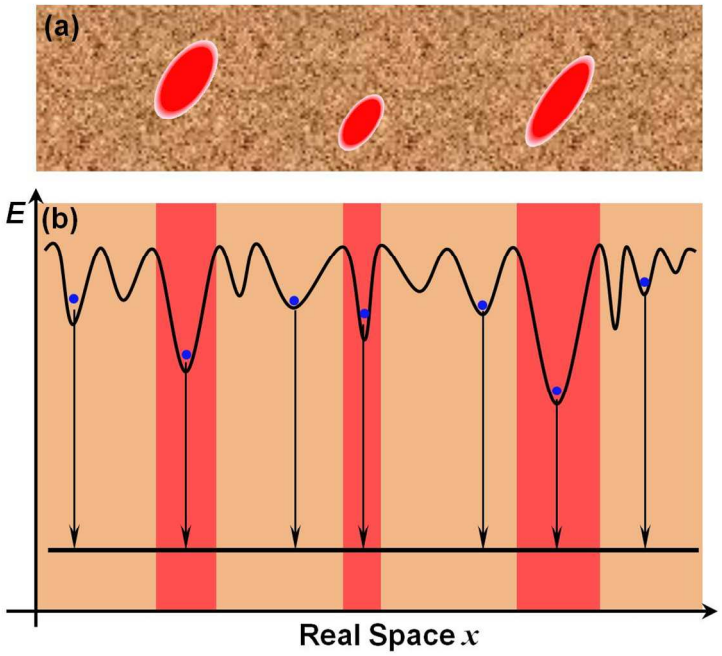

Fig. 5. (a) Schematic depiction of $GaInP_2$ alloy where three ordered domains (red) are represented within the surrounding of the disordered region, (b) the representation of the potential energy profiles where the potential wells in the red regions depict the confinement energy profile of the ordered domains and the rest fluctuating potentials depict the situation in the disordered region. The vertical arrows indicate the radiative recombination transitions from the potential wells.

presented above, the almost completely polarized PL can be ascribed to the emission from the ordered domains, and the non-polarized PL to the emission from the disordered regions. One important supporting point to this proposal is the lower energy position of the polarized emissioncompared with the non-polarized one, because the ordering leads to a band gap lowering compared with counterpart random alloys.[5,9] To graph this idea, we schematically draw a situation of ordered domains embedded in the disordered lattice and their corresponding potential energy profiles in Fig.5. As shown in Fig. 5(a), three red elliptical areas are depicted to represent ordered domains with different sizes and

different degrees of ordering. These ordered $GaInP_2$ domains act as a deep localization well for carriers due to their lower energy band gap. The photoexcited carriers can be quantum mechanically confined inside their potential wells. As the spontaneous ordering effect in the ordered domain leads to the splitting of valence band, that is, the lift-up of heavy-hole and light-hole valence band, the emissive transition from the heavy-hole band should give rise to a polarized emission along the ordering plane. In Fig. 5(b), the potential wells in the red areas represent the potential energy profiles of the respective ordered domains. The potential profile for each ordered domain connects intrinsically with both the size and the degree of ordering. The variation in size and degree of ordering of ordered domains in a real sample will thus lead to a distribution of potential energies which determines the spectral width of the emission of carriers localized in the ordered domains, i.e., the p-PL band. Since neither the size nor the degree of ordering is temperature sensitive, the polarized emission band is expected to broaden insignificantly as the temperature increases. Indeed, as observed in Fig. 4(a), the polarized $I_{p\text{-}PL}$ spectrum shows a much lower broadening rate compared with the $I_{np\text{-}PL}$ counterpart. In contrast to the ordered domains, the disordered region exhibits a broad fluctuating potential profile due to the composition and strain fluctuations in alloy systems. Such fluctuating potential profile can be viewed as a collection of many shallow localization centers for carriers, as schematically depicted in Fig. 5(b), which is characterized with a very broad distribution of density of states. It is not difficult to predict that the emission band from so many such shallow centers caused by disordered atom arrangements should be non-polarized. At the same time, it should be more sensitive to temperature because of much easier thermal re-distribution of carriers within these shallow centers.

This two-type localization state model can also explain the temperature dependence of the relative PL intensity between p-PL and np-PL components, in terms of carrier thermal dynamics. As shown in Fig. 4(b), below the temperature of 20 K, both the $I_{p\text{-}PL}$ and $I_{np\text{-}PL}$ spectra show no observable reduction in intensity. This phenomenon can be attributed to the thermal activation and weak redistribution of localized carriers only inside the respective ordered and disordered alloy domains. At these low temperatures <20 K, the localized-state ensemble luminescence model[17, 18] can be used to do a very good theoretical fitting to the measured PL lines, as shown in Fig. 2(a). For good fitting, two set of main parameters should be used for the polarized and non-polarized PL spectra, indicating two types of carrier localization mechanisms inside the respective disordered and ordered domains. As the temperature is increased beyond 20 K, both the PL intensities start decreasing, but experience different decrease rates as shown in Fig. 4(b). This means that the thermal quenching begins at 20 K for both the PL components. As seen in Fig. 4(b) and discussed previously, the thermal quenching rate of the $I_{p\text{-}PL}$ component is faster than that of the $I_{np\text{-}PL}$ counterpart. Since the two types of carrier localizations occur in the same material, thermal transfer of localized carriers from the ordered domains with deeper localization depth to the disordered regions with shallower

average localization depth could take place and would be more efficient as the temperature increases. To get an in-depth understanding to the mechanism, the integrated PL intensity ratio of $I_{np\text{-}PL}/I_{p\text{-}PL}$ is depicted in the inset of Fig. 4(b) against the inverse of temperature. In terms of thermal activation energy, a temperature dependence of the intensity ratio $I_{p\text{-}PL}/I_{np\text{-}PL}$ can be formulated as[22, 23]

$$\frac{I_{p-PL}}{I_{np-PL}} = C\exp\left(E_A / k_B T\right), \qquad (2)$$

where the factor C is a constant, k_B the Boltzmann constant, and E_A the activation energy. The physical meaning of E_A is the energy difference between the averaged potential depth in the ordered domains and that in the disordered domains, which could be a measure of the thermal transfer probability of the localized carriers from the ordered domains to the disordered regions. The solid line in the inset of Fig. 4(b) is the fitting line by using Eq. (2), and a value of 10 meV was obtained for E_A. This thermal activation energy is reasonable for the $GaInP_2$ materials.[24] So far all the keyexperimental results can be explained reasonably by using the potential energy model considering both kinds of potential wells caused by ordered domains and disordered lattice structures. Our present work shows that, in analyzing polarized PL spectra, their spectral lineshape might contain more information about the physical mechanism and thus we should pay more attention to them. We also want to note that this two-type localization state model may be applicable to other alloy materials with spontaneously ordering effects and even self-assembled quantum dots.

Conclusions

By analyzing the variable-temperature polarized PL spectra of the $GaInP_2$ alloy film grown on GaAs substrate, we show the double-component nature of the PL spectra from $GaInP_2$ alloy with spontaneous atomic ordering. Furthermore, the polarized and non-polarized components of the PL bands are identified to be from the radiative recombination of carriers localized in the ordered domains and disordered lattice regions, respectively. A two-type localization state model capturing the micro-structural nature of ordered $GaInP_2$ domains embedded in a disordered matrixis proposed to interpret the PL spectral features as well as temperature dependent behaviors. This model could be ageneral model for analyzing polarized PL spectra in various alloy materials with spontaneous ordering properties.

Acknowledgements

The study was supported by Natural Science Foundation of China (NSFC) Grants (Grant No. 11374247), the University Development Fund and the SRT on New Materials of HKU, as well as HK-UGC AoE Grants (Project No.: AoE/P-03/08).

References

1 K. H. Huang, J. G. Yu, C. P. Kuo, R. M. Fletcher, T. D. Osentowski, L. J. Stinson, M. G. Craford and A. S. H. Liao, *Appl. Phys. Lett.*, **1992**, 61, 1045; Hiroki Hamada, M. Shono, S. Honda, R. Hiroyama, Keiichi Yodoshi and Takao Yamaguchi, *IEEE J.Quantum Elect.*, **1991**, 27, 1483.

2 H. Fujii, Y. Ueno, A. Gomyo, K. Endo and T. Suzuki, *Appl. Phys. Lett.*, **1992**, 61, 737.

3 K. A. Bertness, Sarah R. Kurtz, D. J. Friedman, A. E. Kibbler, C. Kramer and J. M. Olson, *Appl. Phys. Lett.*, **1994**, 65, 989; R. R. King, D. C. Law, K. M. Edmondson, C. M. Fetzer, G. S. Kinsey, H. Yoon, R. A. Sherif and N. H. Karam, *Appl. Phys. Lett.*, **2007**, 90, 183516; Z. Deng, R. X. Wang, J. Q. Ning, C. C. Zheng, W. Bao, S. J. Xu, X. D. Zhang, S. L. Lu, J. R. Dong, B. S. Zhang and H. Yang, *Sol. Energy Mater. Sol. Cells*, **2013**, 111, 102.

4 P. Bellon, J. P. Chevalier, E. Augarde, J. P. André and G. P. Martin, *J. Appl. Phys.*, **1989**, 66, 2388;G. B. Stringfellow and G. S. Chen, *J. Vac. Sci.Tech. B*, **1991**, 9 , 2182; C. S. Baxter and W. M. Stobbs, *Philos. Mag. A*, **1994**, 69, 615; A. Gomyo, T. Suzuki and S. Iijima, *Phys. Rev. Lett.*, **1988**, 60, 2645.

5 G. S. Horner, A. Mascarenhas, S. Froyen, R. G. Alonso, K. Bertness and J. M. Olson, *Phys. Rev. B*, **1993**, 47, 4041.

6 R. G. Alonso, A. Mascarenhas, S. Froyen, G. S. Horner, K. Bertness and J. M. Olson, *Solid State Commun.*, **1993**, 85, 1021.

7 S. Smith, H. M. Cheong, B. D. Fluegel, J. F. Geisz, J. M. Olson, L. L. Kazmerski and A. Mascarenhas, *Appl. Phys. Lett.*, **1999**, 74, 706; H. M. Cheong, A. Mascarenhas, J. F. Geisz, J. M. Olson, Mark W. Keller and J. R. Wendt, *Phys. Rev. B*, **1998**, 57, R9400.

8 S. H. Wei, D. B. Laks and A. Zunger, *Appl. Phys. Lett.*, **1993**, 62, 1937; S.H. Wei and A. Zunger, *Appl. Phys. Lett.*, **1990**, 56, 662;R. G. Alonso, A. Mascarenhas, G. S. Horner, K. A. Bertness, S. R. Kurtz and J. M. Olson, *Phys. Rev. B*, **1993**, 48, 11833; F. Alsina, N. Mestres, J. Pascual, C. Geng, P. Ernst and F. Scholz, *Phys. Rev. B*, **1996**, 53, 12994; S. H. Wei and A. Zunger, *Phys. Rev. B*,**1994**, 49, 14337;S. H. Wei and A. Zunger, *Phys. Rev. B*, **1998**, 57, 8983;D. B. Laks, S. H. Wei and A. Zunger, *Phys. Rev. Lett.*, **1992**, 69, 3766.

9 S. H. Wei and A. Zunger, *Phys. Rev. B*, **1989**, 39, 3279.

10 S. H. Wei and A. Zunger, *Appl. Phys. Lett.*, **1994**, 64, 757; P. Ernst, Y. Zhang, F. Driessen, A. Mascarenhas, E. D. Jones, C. Geng, F. Scholz and H. Schweizer, *J. Appl. Phys.*, **1997**, 81, 2814; J. S. Luo, J. M. Olson, Sarah R. Kurtz, D. J. Arent, K. A. Bertness, M. E. Raikh and E. V. Tsiper, *Phys. Rev. B*, **1995**, 51, 7603.

11 Y. Hsu, G. B. Stringfellow, C. E. Inglefield, M. C. DeLong, P. C. Taylor, J. H. Cho and T.Y. Seong, *Appl. Phys. Lett.*, **1998**, 73, 3905; J. D. Perkins, Y. Zhang, J. F. Geisz, W. E. McMahon, J. M. Olson and A. Mascarenhas, *J. Appl. Phys.*, **1998**, 84, 4502; S. Froyen and A. Zunger, *Phys. Rev. B*, **1996**, 53, 4570.

12 G. S. Horner, A. Mascarenhas, R. G. Alonso, S. Froyen, K. A. Bertness and J. M. Olson, *Phys. Rev. B*, **1994**, 49, 1727.

13 D. J. Mowbray, R. A. Hogg, M. S. Skolnick, M. C. DeLong, S. R. Kurtz and J. M. Olson, *Phys. Rev. B*, **1992**, 46, 7232.

14 T. Kanata, M. Nishimoto, H. Nakayama,and T. Nishino, *Phys. Rev. B*, **1992**, 45, 6637.

15 S. H. Wei and A. Zunger, *Appl. Phys. Lett.*, **1994**, 64, 1676; P. Ernst, C. Geng, F. Scholz and H. Schweizer, *Phys.Status Solidi B*, **1996**, 193, 213.

16 S. J. Xu, W. Liu and M. F. Li, *Appl. Phys. Lett.*, **2000**, 77, 3376.

17 S. J. Xu, Q. Li, J.R. Dong and S. J. Chua, *Appl. Phys. Lett.*, **2004**, 84, 2280.
18 Q. Li, S. J. Xu, W. C. Cheng, M. H. Xie, S. Y. Tong, C. M. Che and H. Yang, *Appl. Phys. Lett.*, **2001**, 79, 1810; Q. Li, S. J. Xu, M. H. Xie and S. Y. Tong, *Eur. Phys. Lett.*, **2005**, 71, 994.
19 C. M. Fetzer, R. T. Lee, S. W. Jun, G. B. Stringfellow, S. M. Lee and T. Y. Seong, *Appl. Phys. Lett.*, **2001**, 78, 1376; G. S. Horner, A. Mascarenhas, R. G. Alonso, D. J. Friedman, K. Sinha, K. A. Bertness, J. G. Zhu and J. M. Olson, *Phys. Rev. B*, **1993**, 48, 4944.
20 G. Oelgart, A. Knauer, A. Oster and M. Weyers, *J. Appl. Phys.*, **1998**, 84, 1588.
21 G. P. Konnen, *Polarized Light in Nature*, Cambridge University Press, Cambridge, UK, **1985**.
22 Z. Y. Xu, Z. D. Lu, X. P. Yang, Z. L. Yuan, B. Z. Zheng, J. Z. Xu,W. K. Ge, Y. Wang, J. Wang and L. L. Chang, *Phys. Rev. B*, **1996**, 54, 11528.
23 G. Bacherm, C. Hartmann, H. Schweizer, T. Held, G. Mahler and H. Nickel, *Phys. Rev. B*, **1993**, 47, 9545.
24 J. D. Lambkin, L. Considine, S. Walsh, G. M. O'Connor, C. J. McDonagh and T. J. Glynn, *Appl. Phys. Lett.*, **1994**, 65, 73.